THE JOURNAL OF PHYSICAL CHEMISTRY B

Article

pubs.acs.org/JPCB

Insensitivity of Tryptophan Fluorescence to Local Charge Mutations

J. Nathan Scott† and Patrik R. Callis*

Department of Chemistry and Biochemistry, Montana State University, Bozeman, Montana 59717, United States

Supporting Information

ABSTRACT: The steady state fluorescence spectral maximum (λ_{max}) for tryptophan 140 of Staphylococcal nuclease remains virtually unchanged when nearby charged groups are removed by mutation, even though large electrostatic effects on λ_{max} might be expected. To help understand the underlying mechanism of this curious result, we have modeled λ_{max} with three sets of 50-ns molecular dynamics simulations in explicit water, equilibrated with excited state and with ground state charges. Semiempirical quantum mechanics and independent electrostatic analysis for the wild-type protein and four charge-altering mutants were performed on the chromophore using the coordinates from the simulations. Electrostatic contributions from the nearby charged lysines by themselves contribute 30−90 nm red shifts relative to the gas phase, but in each case, contributions from water create compensating blue shifts that bring the predicted λ_{max} within 2 nm of the experimental value, 332 ± 0.5 nm for all five proteins. Although long-range collective interactions from ordered water make large blue shifts, crucial for determining the steady state λ_{max} for absorption and fluorescence, such blue shifts do not contribute to the amplitude of the time dependent Stokes shift following excitation, which comes from nearby charges and only ∼6 waters tightly networked with those charges. We therefore conclude that for STNase, water and protein effects on the Stokes shift are not separable.

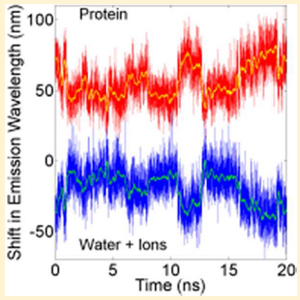

INTRODUCTION

The wavelength of maximum fluorescence intensity (λ_{max}) of the amino acid tryptophan (Trp) is widely exploited in the study of proteins as a probe of electrostatic environment. This environmental sensitivity is theoretically supported by numerous quantum mechanical studies robustly stating that electron density is shifted from the pyrrole ring to the benzene ring during excitation to the ^1L_a state. (For a review, see ref 1.) The sudden charge redistribution causes the surroundings to be transiently out of electrostatic equilibrium, and re-equilibration necessarily causes λ_{max} to shift to longer wavelengths ("red shift") in time scales ranging from ∼50 fs to a few ns. This time-dependent shift is known as the time dependent fluorescence spectral (Stokes) shift or TDFSS. The advent of upconversion methods has provided the ability to observe the evolution of λ_{max} over most of this previously unexplored time window.[2] Much recent activity using ultrafast fluorescence decay methods has been aimed at linking the dynamics of λ_{max} re-equilibration to properties of water near the surface of proteins ("biological water").[3−10] These elegant experiments have established a ubiquitous new phenomenon in which the TDFSS continues to shift over times ranging from 10 ps to over 1 ns.[11,12] A fascinating debate regarding the exact origin of this "slow" relaxation phase has ensued during the decade following its discovery,[5−10,13−24] with the focus often being on the question: does the slow TDFSS report on water dynamics, protein dynamics, or both? Classical molecular dynamics (MD) simulations of the TDFSS typically predict that electrostatic interactions with charged protein groups near the excited Trp contribute significantly, sometimes dominantly.[16,17,20,22,25] A contrasting view holds that the protein environment about an excited Trp is too rigid and inflexible to contribute directly to the TDFSS following excitation by displacement of protein charge to a new equilibrium position relative to the Trp ring.[5,23] The latter view has been driven by the astonishing experimental observation by Qiu et al.[5] that deleting charges close to Trp140 of Staphylococcal nuclease (STNase) by single mutations of Lys133, Lys110, and Glu129 leave the steady state λ_{max} unchanged within experimental error of ±0.5 nm. (Figure 1 shows the relative locations of the mutated charged groups.) This experiment has become an icon for a view which states that the TDFSS reports only water dynamics, albeit assisted by protein dynamics.[5,23] Halle and Nilsson,[15,21] however, have presented a different view, concluding that the 10−100 ps decay does not contain information on protein hydration dynamics.

Most, if not all, previous discussion referenced above has centered on dynamic arguments, aiming to identify whether water or protein is the primary cause of the slow phase of the TDFSS, but here we simulate only the total amplitude of the FSS decay, which is given solely by the Gibbs free energy change (ΔG_{FSS}) associated with the return of the initially excited state to an equilibrium appropriate to the excited state charge distribution. To help understand the invariance of λ_{max} of STNase, we report here predictions of λ_{max} from 50-ns *equilibrium* MD + semiempirical quantum mechanics (QM) ground and excited state simulations for the unmutated (WT) protein and the four mutants for which the nearby lysines and glutamate are changed to neutral amino acids. The purpose of this study is simply to answer two questions: (1) whether MD-

Received: April 27, 2013
Revised: July 23, 2013
Published: July 24, 2013

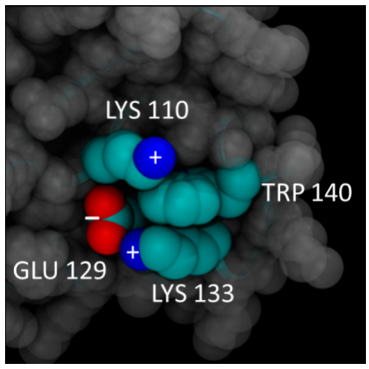

Figure 1. CPK rendering of wild-type Staphylococcal nuclease with key residues labeled and charge indicated. Excitation to the excited state shifts electron density to the benzyl ring (left side of the Trp in this figure), meaning that the Lys residues cause a large stabilization of the excited state (cause a large red shift), whereas Glu129 causes a destabilization of the excited state. The net effect of K133A, K110A, and E129A mutations, along with the concomitant perturbation to water structure, are the focus of this study.

based methods reliably account for the invariance of steady state λ_{max} under local charge state mutations, and (2) whether protein repositioning is predicted to be a significant part of the total change in λ_{max} *following* excitation, which we denote as total TDFSS amplitude.

METHODS

We refer to the hybrid molecular dynamics simulations in explicit water combined with semiempirical quantum mechanics as MD + QM because the QM is not part of dynamics, but is run asynchronously using MD coordinate frames produced earlier. The method used is closely related to that described in detail previously,[25−28] except that the ground state MD simulations were performed using Gromacs 4.5.4[29] with the CHARMM27 all-atom force field.[30] A slightly modified version of the CHARMM27 forcefield was used for excited state simulations, wherein the Trp residue of the forcefield had its atomic charges modified to reflect the Zindo Lowdin excited state charge distribution multiplied by 0.80, which we also provided to Toptygin et al.[22] The QM method is Zerner's spectroscopically calibrated INDO/S-CIS method,[31] incorporating a modification that allows for input of electrostatic potentials and fields developed previously and applied successfully in several earlier studies,[25,26,32−35] and which was based on Zerner's original code for the point charge option. At each point in the trajectory, a QM calculation is done on a reference structure of 3-methylindole (3MI) in the ^1L_a geometry fit to the coordinates of the Trp determined by the MD and experiencing an electrostatic environment given by point charges from all non-QM atoms.

A 1.7 Å crystal structure for the protein STNase, 1STN, was obtained from the RCSB Protein Data Bank.[36] Computationally constructed mutants E129A, K110A, K110C, and K133A of STNase were prepared using the mutate function in Swiss PDB Viewer 4.03,[37] with the lowest energy side chain rotamer selected for the K110C mutant. Crystallographic water oxygen atoms were retained during this processing step so as to be included in the dynamics.

A much more detailed description of the method may be found in the Supporting Information, SI.

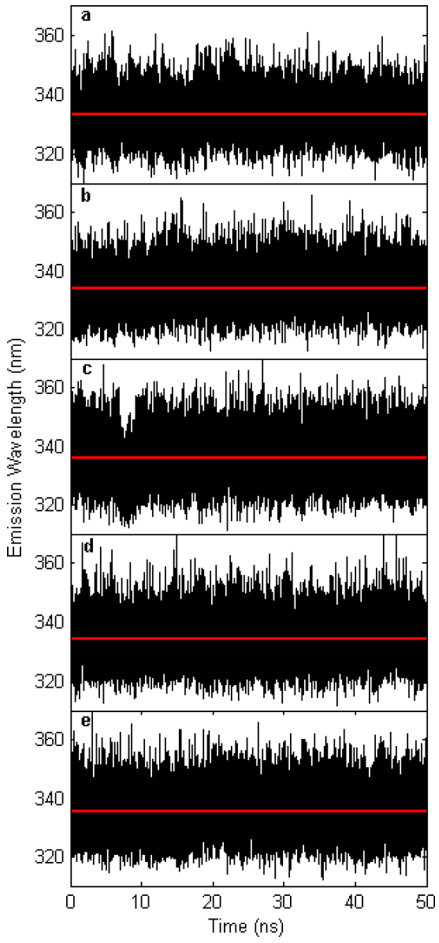

Figure 2. QM + MD trajectories of Ground→ ^1L_a transition energies from representative 50 ns simulations while the Trp charges are fixed at the average value for the *excited state*. In order from top to bottom: WT, K133A, K110A, K110C, and E129A. The heavy red lines are the mean computed λ_{max} values. The fluctuations are due only to environmental electrostatic interactions.

RESULTS

Figure 2 presents 5 MD+QM trajectories of Ground → ^1L_a transition energies from the 50 ns simulations, wherein the 3MI chromophore fragment charges are fixed at the average value for the excited state. One can see that these trajectories, in which the transition energy reflects modification of the Fock Hamiltonian diagonal elements by adding the Coulomb potential energy from all non 3MI atoms of the protein and water system, give nearly the same average value. The λ_{max} values at each frame of the simulation are computed using a geometry determined for the ^1L_a state. The mean values of the λ_{max} values, averaged over 3 independent 50 ns trajectories, are summarized in Table 1. Also in Table 1 are "wavelength shift" contributions computed separately from the Coulomb potentials at chromophore atoms as described in the SI for protein, water, ions, and the sum of these. "Wavelength shift" is actually the electrostatic *energy* difference upon changing from the ground state atomic charges to excited state atomic charges, but is expressed as nm by dividing the value in cm^{-1} by 100. This linearization is exact only at 316.3 nm, but is in error by <11% over the range relevant in this work.

To present the average values from Figure 2 more precisely, Figure 3 shows the results of Figure 2 as the average steady

dx.doi.org/10.1021/jp4041716 | J. Phys. Chem. B 2013, 117, 9598−9605

Table 1. Wavelength Shifts (nm) Broken into Contributions from Protein, Water, Ions and Total from Three 50 ns MD Simulations + QM with Excited State Charges[a]

	protein	water	ions	total	MD + QM wavelength
E129A	76.5 ± 3.3	−28.2 ± 1.1	−10.6 ± 1.4	37.6 ± 1.2	334.3 ± 0.9
WT	58.2 ± 1.3	−13.1 ± 1.8	−7.7 ± 0.4	37.4 ± 0.2	334.3 ± 0.2
K133A	35.2 ± 2.8	10.7 ± 3.1	−6.2 ± 0.6	39.7 ± 0.2	335.9 ± 0.1
K110A	30.1 ± 1.6	11.3 ± 0.2	−5.4 ± 0.6	36.1 ± 1.0	333.3 ± 0.8
K110C	33.8 ± 1.9	10 ± 0.9	−5.6 ± 0.1	38.2 ± 1.0	334.9 ± 0.8

[a]All units are "nm" as given by cm^{-1} /100 except for MD + QM.

state MD + QM computed λ_{max} averaged over the 3 50-ns trajectories for WT and the 4 mutants (red circles) compared to the reported experimental steady state λ_{max} (black squares). Despite the large local differences in electrostatic perturbation from water and protein, the predicted λ_{max} values differ by only ∼2 nm with a standard deviation of ∼4 nm, the expected precision of the method.

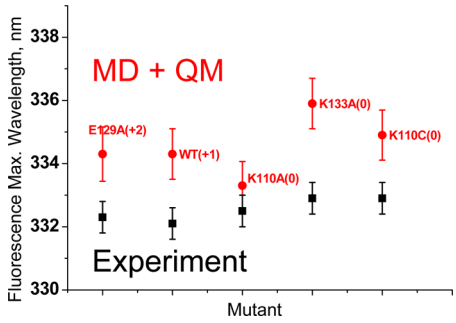

Figure 3. Plot of calculated (red filled circles) and experimental (black squares) tryptophan fluorescence wavelength maxima and standard deviations for the wild-type and the four mutated proteins of this study. In parentheses is the net charge in close proximity to the tryptophan. The red points are mean values of 3 independent 50-ns MD + QM trajectories.

Figure 4 shows that the dielectric compensation leading to invariance of the steady state Stokes shift also has a striking presence in the dynamics.

The rapid fluctuations in contributions from protein (red) and water + ions (blue) to the instantaneous vertical transition energy are seen to be highly anticorrelated during representative 50 ns trajectories for WT and the 4 mutants with the MD system equilibrated to excited state charges. The mean values of the protein and water + ion trajectories in Figure 4 are therefore close to the numbers in Table 1, and sums of these are essentially the red points of Figure 3. The panels shown are ordered top to bottom by the net charge in the Trp pocket.

Figure 5 summarizes the results of Figures 2−4 and Table 1, showing the dissection of the FSS into contributions from protein (red), water (blue), ions (olive), and the total of these three (black) for each of the proteins studied. Also indicated in the boxes is the net charge in close proximity of the Trp, which appears to be a key determinant.

This figure shows clearly that the invariance of the steady state FSS is linked to strong dielectric compensation. That is, removal of charged protein groups near Trp 140 results naturally in an oppositely signed compensation by the bulk water. For WT, protein is seen to contribute a red shift of nearly 60 nm but water contributes a blue shift of 13 nm arising from approximately 200 waters at distances out to 15 Å that are collectively ordered by the positive charge near the Trp. These

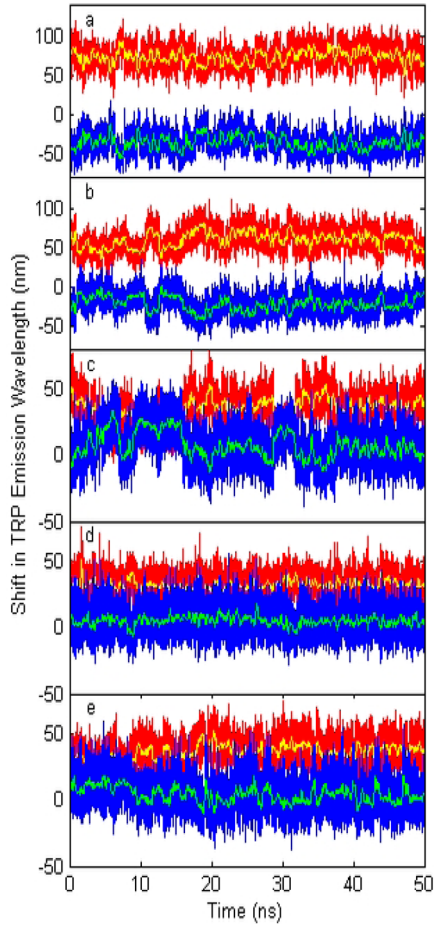

Figure 4. Typical 50 ns trajectories showing anticorrelation of instantaneous wavelength shift contributions from protein (red) and water + ions (blue) for the ground→ ^1L_a transition charge differences when the MD system is equilibrated to *excited state* charges on the Trp for WT STN, and variants: (a) E129A, (b) WT, (c) K133A, (d) K110A, and (e) K110C. The mean values of these trajectories are close to those in Table 1.

numbers are similar to those found in an earlier, less extensive study.[25] Replacing the negatively charged Glu129 with alanine to create the mutant E129A increases the red shift due to protein by ∼20 nm, almost all of which is compensated by an increased blue shift from water. Replacing either Lys133 or Lys110 with a neutral group (alanine or cysteine) reduces the red shift from protein by ∼25 nm while increasing the water contribution by ∼25 to a 10 nm red shift, which again nearly compensates the reduced red shift from protein.

Total TDFSS Amplitude. To this point, all wavelength shifts have been for a chromophore environment fully relaxed and in equilibrium with the excited state charges. The shifts in

dx.doi.org/10.1021/jp4041716 | J. Phys. Chem. B 2013, 117, 9598−9605

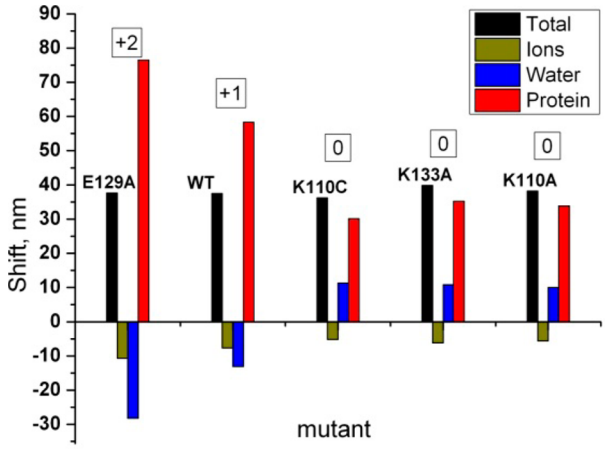

Figure 5. Averaged contributions to the wavelength shift from protein (red), water (blue), ions (olive), and the total of these three (black) with the environment equilibrated to chromophore *excited state* charges for each of the proteins studied. Also indicated in the boxes is the net charge in close proximity to the tryptophan, which appears to be a key determinant in the relative contributions of protein and water.

Table 1 by protein and water are relative to having no environment, i.e., gas phase. The TDFSS measured in ultrafast experiments, however, begins at the instant of excitation, i.e., when the system is equilibrated with the chromophore ground state charges. The focus of this work is therefore on the ΔG for relaxation *following excitation*. To this end, we show in Table 2 the corresponding contributions from protein, water, and ions (averaged from 3 50-ns simulations of WT and the four variants) in which the Trp charges are those for the *ground* state, and in Table 3 the difference of Tables 1 and 2.

In Table 2, the charges are those with which the protein/solvent environment is in equilibrium immediately before excitation. The permanent dipole is much smaller for the ground state than for the ^1L_a state, but has roughly the same direction. For this reason, water uniformly has an even more blue shifting contribution to the FSS when Trp is in the ground state. To compare the equilibrium contributions for the two states, Table 3 and Figure 6 show the difference of Tables 1 and 2, i.e., the difference of electrostatic contributions to the FSS upon going from being equilibrated with ground state to being equilibrated with excited state charges. The numbers in Table 3 should correspond to the total amplitude of the TDFSS observed experimentally.

Figure 6 shows the contributions to the wavelength shift *following* excitation from protein (red), water (blue), and total of water + protein (black) for each of the proteins studied, showing clearly that the equilibrium contributions in the excited state are all more positive than those in Table 2 for the ground state. That is, even though water is often producing a net blue shift before and after relaxation, the blue shift following relaxation is less negative than before relaxation. Most pertinent to this work is that protein makes contributions comparable to or exceeding that from water in all cases. In each of the four cases, the compensating effect of changed water polarization appropriately cancels the large Coulombic perturbation from the nearby charged side chains, leaving the computed total FSS *following excitation* unchanged within the error of the method.

Obviously, the nearby charged groups will individually tend to dominate contributions from protein, but it is of interest to know whether collective effects from more distant charged groups or nearby polar uncharged groups are important. Figure 7 shows the contributions of all individual amino acid residues to the total change in fluorescence Stokes shift following excitation. (In other words, the bars indicate the *difference* between a residue contribution to the FSS in excited and ground state.) Here, and in Figures 8 and 9, distance from Trp is calculated as the average of all intermolecular atom−atom distances between a residue or water and the Trp chromophore (indole ring atoms and Cβ). Note that the nearby Lys133 and Lys110, which sandwich Trp140 and exhibit large amplitude fluctuations in position, are dominant in producing contributions to a net red shift. Somewhat surprising is that we find ∼40% of the shift from these lysines originates from the hydrocarbon chains, which are in van der Waals contact with the indole ring most of the time. Because there is extensive cancellation of the many other contributions, the sum of electrostatic contributions from the shift due to Lys110 and Lys133 is very nearly the same as the total shift from protein. The negatively charged Glu129 has a smaller, negative (blue shift) effect, even though quite close, probably because it is often locked more rigidly in place by H-bonds to Arg126 and Val111. Lysines 116 and 48, though ∼25 Å distant, contribute ∼1 nm red shifts primarily through azimuthal position changes because their radius vector from Trp is ∼45 degrees. Thus, Figure 7 illustrates the complexity possible in the overall contribution from protein to the FSS.

We constructed histograms of water contributions by distance at 0.01 Å intervals to determine the distances at which water is active in producing the total TDFSS. Figure 8 shows the integrated equilibrium Stokes shifts from water in ground (blue) and excited (red) states, as a function of average distance from the Trp. That is, the shift at a given distance from Trp is the sum of shifts from all waters at that distance or closer. Waters more distant than 5.7 Å from Trp on average contribute nearly the same destabilization to both ground and excited states, and therefore contributed negligibly to the total TDFSS amplitude.

Figure 9 shows the difference of the excited and ground state curves of Figure 8. It is seen that only about 6 water molecules located closer than ∼6 Å from Trp contribute to the total TDFSS. The red curve shows the average contribution per

Table 2. Wavelength Shifts (nm) Broken into Contributions from Protein, Water, Ions and Total from Three 50 ns MD Simulations + QM with *Ground* State Charges

	protein	water	ions	total	MD + QM wavelength
E129A	55.9 ± 3.5	−38.5 ± 2.5	−9 ± 1.1	8.5 ± 1.5	314.2 ± 0.8
WT	38.3 ± 4.4	−22 ± 4.5	−6 ± 0.4	10.3 ± 0.5	315.1 ± 0.3
K133A	23.4 ± 0.5	−9.9 ± 0.7	−4.3 ± 0.4	9.2 ± 0.2	314.7 ± 0.1
K110A	16 ± 0.1	−3 ± 0.3	−4 ± 0.3	9 ± 0.2	314.5 ± 0.0
K110C	18.6 ± 0.8	−5.5 ± 1.1	−4.1 ± 0.4	8.9 ± 0.2	314.4 ± 0.1

dx.doi.org/10.1021/jp4041716 | J. Phys. Chem. B 2013, 117, 9598−9605

Table 3. Total Steady State Stokes Shift (nm) Following *Excitation*, Given by the Difference of Tables 1 and 2

	protein	water	ions	total	MD + QM shift
E129A	20.6 ± 4.8	10.2 ± 2.7	−1.7 ± 1.7	29.1 ± 1.9	20.1 ± 1.2
WT	20 ± 4.6	8.9 ± 4.9	−1.7 ± 0.6	27.1 ± 0.6	19.1 ± 0.3
K133A	11.8 ± 2.8	20.6 ± 3.2	−1.9 ± 0.7	30.5 ± 0.2	21.1 ± 0.1
K110A	14.2 ± 1.6	14.2 ± 0.4	−1.3 ± 0.7	27.1 ± 1.0	18.9 ± 0.8
K110C	15.2 ± 2.0	15.6 ± 1.4	−1.5 ± 0.4	29.3 ± 1.0	20.5 ± 0.8

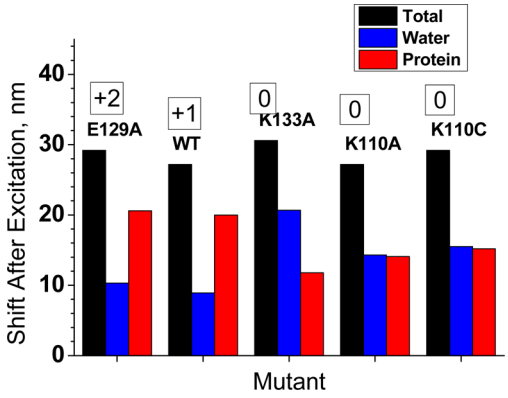

Figure 6. Contributions to the total TDFSS (the change in fluorescence wavelength *following excitation*) from protein (red), water (blue), and total of water + protein (black) for each of the proteins studied. Also indicated in the boxes are the net charges in close proximity to the tryptophan.

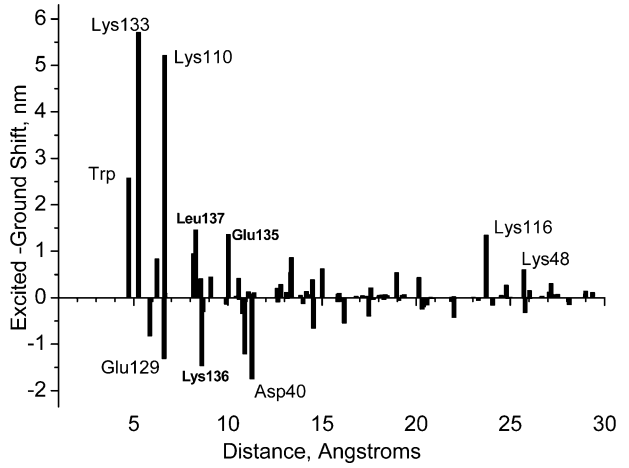

Figure 7. Contribution of individual WT protein residues to total change in fluorescence Stokes shift *following excitation*. The bars indicate the difference between individual residue contributions to wavelength in the excited and ground state. The nearby Lys133 and Lys110 are dominant in producing contributions to a net red shift.

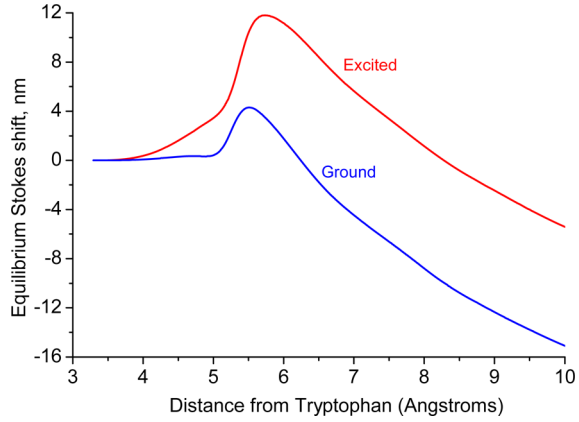

Figure 8. Integrated equilibrium Stokes shifts from water in ground (blue) and excited (red) states for the WT protein. The shift at a given distance from Trp is the sum from all waters at that distance or closer. Waters more distant than 5.7 Å from Trp on average contribute blue shifts, which are nearly independent of excitation.

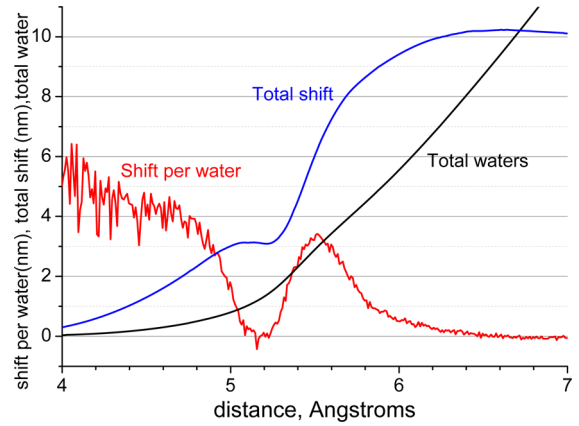

Figure 9. Waters that contribute to the total TDFSS amplitude (Stokes shift *following excitation*) shown in Figure 6 for WT as a function of mean distance from Trp140: average contribution per water at 0.01 Å resolution (red); total shift contributed by all waters within distance on abscissa from Trp140 (blue); and total number of waters on average found within distance on abscissa from Trp140 (black).

water at 0.01 Å resolution as a function of distance from Trp, and the blue curve gives the total shift contributed by all water within a given distance from Trp. The black curve gives the total number of waters on average found within a given distance from Trp, which was the essentially the same for ground and excited states. On average, only one water molecule at a distance <5.2 Å from Trp makes a 3 nm contribution to the total FSS, and about 5 waters between 5.2 and 6.2 Å contribute 7 nm.

DISCUSSION

Recalling that a primary focus of this work is to understand the invariance under local charge state mutations of the steady state λ_{max}, which is effectively an equilibrium property, we are concerned with the change in free energy, ΔG_{FSS}, for the system to return to equilibrium following excitation. Because of the large increase in permanent dipole, the entire chromophore−protein−water system is in a nonequilibrium state at the instant following light absorption during a vertical transition between ground (0) and excited (1) state. The relation

dx.doi.org/10.1021/jp4041716 | J. Phys. Chem. B 2013, 117, 9598−9605

between the equilibrium λ_{max} and ΔG_{FSS} was first established by Marcus in a remarkable series of single-author papers,[38−43] which formally connected the electrostatic free energy of such a nonequilibrium state relative to its equivalent (ultimately relaxed) equilibrium state, $G^{non}-G_1$, i.e., the reorganization energy, λ_{reorg} (not a wavelength). The expression for λ_{reorg}, which is the same as defined in the well-known Marcus electron transfer theory when electron transfer is considered instantaneous, was shown to be given by eq 1,

$$\lambda_{reorg} = G^{non} - G_1^{eq} = G_{1-0}^{op,eq} - G_{1-0}^{eq} = \Delta G_{FSS} \quad (1)$$

where the quantity G^{eq}_{1-0} refers to a fictitious electrostatic free energy of a molecule with charge density equal to the *difference* of the charge densities of the ground and excited states in equilibrium with its surroundings. $G^{op,eq}_{1-0}$ is the equivalent quantity in equilibrium with the same surroundings, with the exception of being spatially frozen so that only the electronic (optical) polarizability can respond to the 1−0 electron density change, which instantly establishes equilibrium with the solute at the time of the electronic excitation. Therefore, the free energy change associated with the total FSS *following excitation* is the total free energy change minus that which would be provided by only the electronic polarizability of the surroundings. Fortunately, this is what we and virtually all published MD simulations seeking to compute FSS have used, regardless of whether quantum chemical calculations were involved.[15−17,20−22,25]

Next we examine what our MD + QM computations say regarding protein contributions to ΔG_{FSS}, i.e., the total TDFSS amplitude. Given that the average positions of Lys133 and Lys110 lie above and below the benzene end of the indole ring, and that electron density is transferred from the pyrrole ring to the benzene ring during excitation, Coulomb's Law says that the positively charged Lys ammonium groups alone contribute an extremely large negative change in electrostatic energy upon excitation (contribute a large red shift). There is a correspondingly strong force of attraction to move the lysines closer to the benzene ring. If unhindered, then the positive ammonium groups would clearly move under this force and contribute further to the FSS. The rather fluid nature of the positively charged ammonium groups on the lysines, which are on the end of flexible alkane chains, does indeed allow these nearby charges to respond significantly to the sudden Coulombic field created by excitation. In addition, the ammonium group is strongly hydrogen bonded to the oxygens of 3 waters. The N−H bonds point outward toward the bulk solvent and away from the benzene ring so that the dipole of the attached waters is repelled on average by the large excited state dipole on the Trp. These waters therefore contribute a positive electrostatic energy (blue shift) to the FSS, partially canceling that from the lysines, and also opposing the force that would draw the lysines to the benzene ring of the Trp. These three waters in turn are H-bonded to waters in the next solvation shell, establishing thereby a series of "water wires" that remain somewhat ordered out into the solvent. Cancellation is not 100% because the waters are mostly farther from the Trp than are the lysines, thus leading to a FSS that is dominated by Lys133 and 110. For this reason—and because of the diversity of protein vs water contributions reported from other work—we believe it is not correct to state that protein never plays a direct role in the TDFSS amplitude.

Dynamic Information. Dynamic information is provided by the fluctuations of protein and water electrostatic contributions found in the simulations used to establish the ground and excited state equilibrium properties (Figure 4). The large, rapid fluctuations in protein and water contributions are anticorrelated so tightly—within nearly the fastest response times of water (∼100 fs)—that we cannot discern whether water, protein, or both are driving the fluctuations. Anticorrelation of this nature has been reported as part of numerous studies, and exhibits great diversity in terms of protein-water contributions in different proteins.[15−18,20,21,24−26,44] The tight coupling of the Lys ammonium groups and water described above is most likely responsible for most of this anticorrelation. This is strongly reinforced by our finding that only about 6 waters within ∼6 A of Trp are responsible for producing the total FSS beyond what is provided by the protein. Graphical examination of individual frames from the MD simulations confirms this conclusion. The picture that emerges from these findings is that, for this protein, those few waters and protein groups contributing significantly to the total TDFSS are intimately connected. Whether protein or water dominates the slow phase of the TDFSS does not appear to be a meaningful question.

■ CONCLUSIONS

MD + QM simulations show that protein charges positioned close to Trp140 in STNase near the surface of the protein that create an ultra large fluorescence wavelength shift according to Coulomb's Law, also create a strongly polarized hydration shell out to ∼15 Å that dielectrically opposes the protein effect (dielectric compensation). Mutations that change the charge environment near Trp therefore have only a very small effect on the wavelength maximum, in agreement with experiment. Thus, while it may seem unlikely that mutations at three different sites would exactly cancel the effect of hydration and protein solvation to give nearly the same Stokes shifts and correlation functions, straightforward application of MD simulations clearly shows that this is not simply fortuitous. This finding is essentially the view presented by Halle and Nilsson.[15,21]

In addition, the rather fluid nature of the positively charged ammonium groups on the lysines, which are on the end of flexible alkane chains, allows these nearby charges to respond to the sudden Coulombic field created by excitation, in contrast with the supposition presented by Zhong, Zewail, and coworkers, wherein the charged groups near Trp in the STNase protein are packed too rigidly to provide a relaxation contribution to the FSS.[5,23]

The extremely tight anticorrelation we see for WT and E129A is a direct manifestation of the solvent−protein coupling that is often mentioned in connection with the 10−100 ps relaxation,[15,17,20,21] even when the relaxation itself is attributed only to water.[23] The simulations reported here say that protein and water both contribute substantially to λ_{reorg}, and appear to be locked together during fluctuations. We find that not only does protein relaxation contribute considerably to the FSS, but also the only water contribution to the FSS comes from ∼6 waters within 6 Å of Trp, which are part of a tight H-bond network that includes the nearby charges. The motions of the protein and water in this active ensemble are in unison and cannot be separated. For STNase, the protein charges and water that actually contribute to the FSS are so strongly coupled and correlated near the surface of the protein that we believe whether the slow TDFSS is probing water or protein is not a meaningful question for this protein.

dx.doi.org/10.1021/jp4041716 | J. Phys. Chem. B 2013, 117, 9598−9605

■ ASSOCIATED CONTENT

Supporting Information

(1) A more detailed and complete description of the methods; (2) Figure S1 showing correlation of Zindo transition energies with nonquantum mechanical estimates of wavelength shifts; and (3) Figure S2, which is the counterpart of Figure 4 for equilibration with chromophore ground state charges. This material is available free of charge via the Internet at http://pubs.acs.org.

■ AUTHOR INFORMATION

Corresponding Author

*Phone: 406-994-5414; fax: 406-994-5407; e-mail: pcallis@montana.edu.

Present Address

†Department of Chemistry, Saint Francis University, Loretto, PA, 15940, U.S.A.

Notes

The authors declare no competing financial interest.

■ ACKNOWLEDGMENTS

We gratefully acknowledge support for this work from NSF MCB Grant No. 084704. This work used the Extreme Science and Engineering Discovery Environment (XSEDE), which is supported by National Science Foundation Grant No. OCI-1053575 through Project No. MCB090176.

■ REFERENCES

(1) Callis, P. R. ^1L_a and ^1L_b Transitions of Tryptophan: Applications of Theory and Experimental Observations to Fluorescence of Proteins. *Methods Enzymol.* **1997**, *278*, 113−150.

(2) Ruggiero, A. J.; Todd, D. C.; Fleming, G. R. Subpicosecond Fluorescence Anisotropy Studies of Tryptophan in Water. *J. Am. Chem. Soc.* **1990**, *112*, 1003−1014.

(3) Pal, S. K.; Peon, J.; Zewail, A. H. Biological Water at the Protein Surface: Dynamical Solvation Probed Directly With Femtosecond Resolution. *Proc. Natl. Acad. Sci. U.S.A.* **2002**, *99*, 1763−1768.

(4) Peon, J.; Pal, S. K.; Zewail, A. H. Hydration at the Surface of the Protein Monellin: Dynamics With Femtosecond Resolution. *Proc. Natl. Acad. Sci. U.S.A.* **2002**, *99*, 10964−10969.

(5) Qiu, W. H.; Kao, Y. T.; Zhang, L. Y.; Yang, Y.; Wang, L. J.; Stites, W. E.; Zhong, D. P.; Zewail, A. H. Protein Surface Hydration Mapped by Site-Specific Mutations. *Proc. Natl. Acad. Sci. U.S.A.* **2006**, *103*, 13979−13984.

(6) Zhang, L. Y.; Yang, Y.; Kao, Y. T.; Wang, L. J.; Zhong, D. P. Protein Hydration Dynamics and Molecular Mechanism of Coupled Water-Protein Fluctuations. *J. Am. Chem. Soc.* **2009**, *131*, 10677−10691.

(7) Qin, Y. Z.; Chang, C. W.; Wang, L. J.; Zhong, D. P. Validation of Response Function Construction and Probing Heterogeneous Protein Hydration by Intrinsic Tryptophan. *J. Phys. Chem. B* **2012**, *116*, 13320−13330.

(8) Yang, J.; Zhang, L. Y.; Wang, L. J.; Zhong, D. P. Femtosecond Conical Intersection Dynamics of Tryptophan in Proteins and Validation of Slowdown of Hydration Layer Dynamics. *J. Am. Chem. Soc.* **2012**, *134*, 16460−16463.

(9) Bose, S.; Adhikary, R.; Mukherjee, P.; Song, X. Y.; Petrich, J. W. Considerations for the Construction of the Solvation Correlation Function and Implications for the Interpretation of Dielectric Relaxation in Proteins. *J. Phys. Chem. B* **2009**, *113*, 11061−11068.

(10) Bose, S.; Adhikary, R.; Barnes, C. A.; Fulton, D. B.; Hargrove, M. S.; Song, X. Y.; Petrich, J. W. Comparison of the Dielectric Response Obtained From Fluorescence Upconversion Measurements and Molecular Dynamics Simulations for Coumarin 153-Apomyoglobin Complexes and Structural Analysis of the Complexes by NMR and Fluorescence Methods. *J. Phys. Chem. B* **2011**, *115*, 3630−3641.

(11) Toptygin, D.; Savtchenko, R. S.; Meadow, N. D.; Brand, L. Homogeneous Spectrally- and Time-Resolved Fluorescence Emission From Single-Tryptophan Mutants of IIA^{Glc}. *J. Phys. Chem. B* **2001**, *105*, 2043−2055.

(12) Toptygin, D.; Gronenborn, A. M.; Brand, L. Nanosecond Relaxation Dynamics of Protein GB1 Identified by the Time-Dependent Red Shift in the Fluorescence of Tryptophan and 5-Fluorotryptophan. *J. Phys. Chem. B* **2006**, *110*, 26292−26302.

(13) Pal, S. K.; Peon, J.; Bagchi, B.; Zewail, A. H. Biological Water: Femtosecond Dynamics of Macromolecular Hydration. *J. Phys. Chem. B* **2002**, *106*, 12376−12395.

(14) Pal, S. K.; Zewail, A. H. Dynamics of Water in Biological Recognition. *Chem. Rev.* **2004**, *104*, 2099−2123.

(15) Nilsson, L.; Halle, B. Molecular Origin of Time-Dependent Fluorescence Shifts in Proteins. *Proc. Natl. Acad. Sci. U.S.A.* **2005**, *102*, 13867−13872.

(16) Hassanali, A. A.; Li, T. P.; Zhong, D. P.; Singer, S. J. A Molecular Dynamics Study of Lys-Trp-Lys: Structure and Dynamics in Solution Following Photoexcitation. *J. Phys. Chem. B* **2006**, *110*, 10497−10508.

(17) Li, T. P.; Hassanali, A. A. P.; Kao, Y. T.; Zhong, D. P.; Singer, S. J. Hydration Dynamics and Time Scales of Coupled Water-Protein Fluctuations. *J. Am. Chem. Soc.* **2007**, *129*, 3376−3382.

(18) Golosov, A. A.; Karplus, M. Probing Polar Solvation Dynamics in Proteins: A Molecular Dynamics Simulation Analysis. *J. Phys. Chem. B* **2007**, *111*, 1482−1490.

(19) Pizzitutti, F.; Marchi, M.; Sterpone, F.; Rossky, P. J. How Protein Surfaces Induce Anomalous Dynamics of Hydration Water. *J. Phys. Chem. B* **2007**, *111*, 7584−7590.

(20) Li, T. P.; Hassanali, A. A.; Singer, S. J. Origin of Slow Relaxation Following Photoexcitation of W7 in Myoglobin and the Dynamics of Its Hydration Layer. *J. Phys. Chem. B* **2008**, *112*, 16121−16134.

(21) Halle, B.; Nilsson, L. Does the Dynamic Stokes Shift Report on Slow Protein Hydration Dynamics? *J. Phys. Chem. B* **2009**, *113*, 8210−8213.

(22) Toptygin, D.; Woolf, T. B.; Brand, L. Picosecond Protein Dynamics: The Origin of the Time-Dependent Spectral Shift in the Fluorescence of the Single Trp in the Protein GB1. *J. Phys. Chem. B* **2010**, *114*, 11323−11337.

(23) Zhong, D. P.; Pal, S. K.; Zewail, A. H. Biological Water: A Critique. *Chem. Phys. Lett.* **2011**, *503*, 1−11.

(24) Matyushov, D. V. Nanosecond Stokes Shift Dynamics, Dynamical Transition, and Gigantic Reorganization Energy of Hydrated Heme Proteins. *J. Phys. Chem. B* **2011**, *115*, 10715−10724.

(25) Vivian, J. T.; Callis, P. R. Mechanisms of Tryptophan Fluorescence Shifts in Proteins. *Biophys. J.* **2001**, *80*, 2093−2109.

(26) Pan, C. P.; Callis, P. R.; Barkley, M. D. Dependence of Tryptophan Emission Wavelength on Conformation in Cyclic Hexapeptides. *J. Phys. Chem. B* **2006**, *110*, 7009−7016.

(27) Callis, P. R. Predicting Fluorescence Lifetimes and Spectra of Biopolymers. *Methods Enzymol.* **2011**, *487*, 1−38.

(28) Tusell, J. R.; Callis, P. R. Simulations of Tryptophan Fluorescence Dynamics During Folding of the Villin Headpiece. *J. Phys. Chem. B* **2012**, *116*, 2586−2594.

(29) Hess, B.; Kutzner, C.; van der Spoel, D.; Lindahl, E. Algorithms for Highly Efficient, Load-Balanced, and Scalable Molecular Simulation. *J. Chem. Theory Comp.* **2008**, *4*, 435−447.

(30) MacKerell, A. D.; Banavali, N.; Foloppe, N. Development and Current Status of the CHARMM Force Field for Nucleic Acids. *Biopolymers* **2001**, *56*, 257−265.

(31) Ridley, J.; Zerner, M. Intermediate Neglect of Differential Overlap (INDO) Technique for Spectroscopy: Pyrrole and the Azines. *Theor. Chim. Acta (Berlin)* **1973**, *32*, 111−134.

(32) Theiste, D.; Callis, P. R.; Woody, R. W. Effects of the Crystal Field on Transition Moments in 9- Ethylguanine. *J. Am. Chem. Soc.* **1991**, *113*, 3260−3267.

(33) Sreerama, N.; Woody, R. W.; Callis, P. R. Theoretical Study of the Crystal Field Effects on the Transition Dipole Moments in Methylated Adenines. *J. Phys. Chem.* **1994**, *98*, 10397−10407.
(34) Broos, J.; Tveen-Jensen, K.; de Waal, E.; Hesp, B. H.; Jackson, J. B.; Canters, G. W.; Callis, P. R. The Emitting State of Tryptophan in Proteins With Highly Blue-Shifted Fluorescence. *Angew. Chem., Int. Ed.* **2007**, *46*, 5137−5139.
(35) Pan, C. P.; Muino, P. L.; Barkley, M. D.; Callis, P. R. Correlation of Tryptophan Fluorescence Spectral Shifts and Lifetimes Arising Directly From Heterogeneous Environment. *J. Phys. Chem. B* **2011**, *115*, 3245−3253.
(36) Bernstein, F. C.; Koetzle, T. F.; Williams, G. J. B.; Meyer, E. F.; Brice, M. D.; Rodgers, J. R.; Kennard, O.; Shimanouchi, T.; Tasumi, M. Protein Data Bank—Computer-Based Archival File for Macromolecular Structures. *J. Mol. Biol.* **1977**, *112*, 535−542.
(37) Guex, N.; Peitsch, M. C. SWISS-MODEL and the Swiss-PdbViewer: An Environment for Comparative Protein Modeling. *Electrophoresis* **1997**, *18*, 2714−2723.
(38) Marcus, R. A. Electrostatic Free Energy and Other Properties of States Having Nonequilibrium Polarization 0.1. *J. Chem. Phys.* **1956**, *24*, 979−989.
(39) Marcus, R. A. Free Energy of Nonequilibrium Polarization Systems 0.3. Statistical Mechanics of Homogeneous and Electrode Systems. *J. Chem. Phys.* **1963**, *39*, 1734−1740.
(40) Marcus, R. A. Interactions in Polar Media 0.1. Interparticle Interaction Energy. *J. Chem. Phys.* **1963**, *38*, 1335−1340.
(41) Marcus, R. A. On Theory of Shifts and Broadening of Electronic Spectra of Polar Solutes in Polar Media. *J. Chem. Phys.* **1965**, *43*, 1261−1274.
(42) Marcus, R. A. Theory of Oxidation-Reduction Reactions Involving Electron Transfer 0.4. A Statistical-Mechanical Basis for Treating Contributions From Solvent, Ligands, and Inert Salt. *Discuss. Faraday Soc.* **1960**, 21−31.
(43) Marcus, R. A. Reorganization Free-Energy for Electron Transfers at Liquid Liquid and Dielectric Semiconductor Liquid Interfaces. *J. Phys. Chem.* **1990**, *94*, 1050−1055.
(44) Biesso, A.; Muino, P. L.; Xu, J. H.; Callis, P. R.; Knutson, J. Trp Fluorescence in GB1: Nanosecond Dynamics Strongly Depend on pH While 30Ps Relaxation Is Constant. *Biophys. J.* **2013**, *104*, 344A−345A.